Cronfa - Swansea University Open Access Repository

_____

This is an author produced version of a paper published in:
Journal of Geophysical Research: Earth Surface

Cronfa URL for this paper:
http://cronfa.swan.ac.uk/Record/cronfa39611

_____

Paper:

Sevestre, H., Benn, D., Luckman, A., Nuth, C., Kohler, J., Lindbäck, K. & Pettersson, R. (2018). Tidewater Glacier Surges Initiated at the Terminus. _Journal of Geophysical Research: Earth Surface, 123_(5), 1035-1051.
http://dx.doi.org/10.1029/2017JF004358

_____

http://www.swansea.ac.uk/library/researchsupport/ris-support/

RESEARCH ARTICLE

Key Points:
- Patterns of surge propagation of two tidewater glaciers are investigated in unprecedented details
- The initial slow buildup was caused by rising driving stresses and enhanced meltwater production
- The sudden switch to fast flow is caused by surface to bed drainage through up-glacier expanding crevasse fields

Tidewater Glacier Surges Initiated at the Terminus

Heïdi Sevestre[1] [iD], Douglas I. Benn[1] [iD], Adrian Luckman[2,3] [iD], Christopher Nuth[4] [iD], Jack Kohler[5] [iD], Katrin Lindbäck[5], and Rickard Pettersson[6] [iD]

[1]School of Geography and Sustainable Development, University of St Andrews, Saint Andrews, UK, [2]Department of Geography, College of Science, Swansea University, Swansea, UK, [3]Department of Arctic Geophysics, The University Centre in Svalbard, Longyearbyen, Norway, [4]Department of Geosciences, Faculty of Mathematics and Natural Sciences, University of Oslo, Oslo, Norway, [5]Norwegian Polar Institute, Tromsø, Norway, [6]Department of Earth Sciences, Uppsala University, Uppsala, Sweden

Abstract There have been numerous reports that surges of tidewater glaciers in Svalbard were initiated at the terminus and propagated up-glacier, in contrast with downglacier-propagating surges of land-terminating glaciers. Most of these surges were poorly documented, and the cause of this behavior was unknown. We present detailed data on the recent surges of two tidewater glaciers, Aavatsmarkbreen and Wahlenbergbreen, in Svalbard. High-resolution time series of glacier velocities and evolution of crevasse patterns show that both surges propagated up-glacier in abrupt steps. Prior to the surges, both glaciers underwent retreat and steepening, and in the case of Aavatsmarkbreen, we demonstrate that this was accompanied by a large increase in driving stress in the terminal zone. The surges developed in response to two distinct processes. (1) During the late quiescent phase, internal thermodynamic processes and/or retreat from a pinning point caused acceleration of the glacier front, leading to the development of terminal crevasse fields. (2) Crevasses allowed surface meltwater and rainwater to access the bed, causing flow acceleration and development of new crevasses up-glacier. Upward migration of the surge coincided with stepwise expansion of the crevasse field. Geometric changes near the terminus of these glaciers appear to have led to greater strain heating, water production, and storage at the glacier bed. Water routing via crevasses likely plays an important role in the evolution of surges. The distinction between internally triggered surges and externally triggered speedups may not be straightforward. The behavior of these glaciers can be understood in terms of the enthalpy cycle model.

1. Introduction

The classic studies of Variegated Glacier, Trapridge Glacier, and Bakaninbreen (Clarke et al., 1984; Frappé-Sénéclauze & Clarke, 2007; Kamb et al., 1985; Murray et al., 2000) established a "standard surge cycle," during which glaciers exhibit a characteristic quasiperiodic sequence of geometric and dynamic changes. During the quiescent phase, an upper "reservoir zone" thickens and steepens until the surge phase is initiated. From this nucleus, the surge propagates downglacier, with a well-defined surge front marking the boundary between fast-moving ice up-glacier and slow ice downstream. The passage of the bulge compresses ice downglacier, while the ice upstream undergoes extensional stresses. Downglacier propagation of the surge transfers mass to a receiving zone and causes substantial surface drawdown on the upper glacier, thickening of the lower glacier, and possible terminus advance (Meier & Post, 1969).

In Svalbard, however, surges of some tidewater glaciers depart from this standard sequence. While surges of land-terminating glaciers in Svalbard follow the stages described above (Dowdeswell & Benham, 2003; Mansell et al., 2012; Murray et al., 1998; Sund et al., 2009), there are numerous reports of tidewater glacier surges initiating at the terminus and propagating up-glacier. Remote sensing analyses of surges of Osbornebreen (Rolstad et al., 1997), Perseibreen (Dowdeswell & Benham, 2003), Tunabreen (Flink et al., 2015), Monacobreen (Luckman et al., 2002; Murray, Strozzi, et al., 2003), and Fridtjovbreen (Murray, Luckman, et al., 2003; Murray et al., 2012) have clearly demonstrated this pattern, with an up-glacier propagation of the surge accompanied by extensional crevassing. Analyses of crevasse patterns show the absence of a compressive surge bulge in all cases. Studies such as Dunse et al. (2015) revealed the importance of such crevasses in routing surface meltwater to the bed and mobilizing initially frozen regions of the glaciers into the surge.

Many aspects of this class of surges remain poorly known. In particular, it is unclear whether surges of Svalbard tidewater glaciers are driven by similar cyclic internal processes to land-terminating glaciers

(McMillan et al., 2014; Sund et al., 2009), or if they occur in response to changes in the force balance at the terminus, like "speedups" of tidewater glaciers observed in Greenland and elsewhere (Howat et al., 2005; Joughin et al., 2004; Nick et al., 2009). Resolving this issue is difficult, because there is very limited information on the evolution of glaciers prior to their surges. Few velocity data are available, and surges are often already in progress before the start of observations. In the absence of comprehensive velocity data, patterns of surge propagation are largely inferred from proxy data, such as the analysis of crevasse patterns (Flink et al., 2015).

In this paper, we present detailed data on recent surges of two tidewater glaciers in western Svalbard. Svalbard has the densest population of surge-type glaciers in the world (Hagen et al., 1993; Jiskoot et al., 2000; Sevestre & Benn, 2015), and we fortuitously captured velocity data on surges of Aavatsmarkbreen and Wahlenbergbreen as a by-product of a study of calving glaciers in the archipelago (Luckman et al., 2015). High-spatial-resolution velocity fields were obtained for both glaciers from TerraSAR-X images, at about 11-day intervals for a period of 2 years for Wahlenbergbreen and almost 3 years for Aavatsmarkbreen. This spanned the entire surge phase of Aavatsmarkbreen, and the main phase of surge propagation of Wahlenbergbreen. In addition, we reconstructed changes in surface elevation, driving stresses, and crevasse distribution prior to and during the surge of Aavatsmarkbreen. Due to the lack of recent ground-penetrating radar (GPR) data on Wahlenbergbreen, our attention focused on the changes in elevation, evolution of the velocity field and in the extent of the terminal crevasse field. All these data sets combined for both glaciers allowed us to identify the mechanisms of surge initiation and propagation in great detail. Finally, we consider the question of whether surges of land-terminating and tidewater glaciers can be explained within the single conceptual framework of enthalpy budget, despite their differences.

2. Study Areas

2.1. Aavatsmarkbreen

Aavatsmarkbreen (78.70°N 12.29°E) is a 15-km-long tidewater glacier in Oscar II Land, on the north-west coast of Spitsbergen, Svalbard (Figure 1; König et al., 2013; Pfeffer et al., 2014). The glacier flows westward into the bay of Hornbæbukta, where it terminates in a 3-km wide calving front. The glacier is fed by two main accumulation basins reaching a maximum elevation of 834 m above sea level (a.s.l.). Several unnamed minor tributaries join the upper half of the main trunk above 250 m a.s.l. Recent observations at the margins of Aavatsmarkbreen have revealed that the glacier is resting on a thin layer of glacial deposits (up to 0.5 m; Sobota et al., 2016).

There have been two reported advances of Aavatsmarkbreen since the end of the Little Ice Age and prior to the most recent surge of 2013–2015. Niewiarowski (1982) and Lankauf (1999) presented evidence that a rapid advance of the glacier took place between 1909 and 1936–1938, interpreted as a surge on the basis of thrust moraines on both sides of Hornbæbukta as well as changes in elevation of the glacier typical of a surge. No information on the magnitude of the advance of the glacier could be found. A second advance occurred in the early 1980s (Lankauf, 1999). In 1985 the glacier's appearance and geometry had substantially changed relative to that of 1978, and its surface was bulging and intensely crevassed. The terminus advanced as much as 250 m locally. Investigations of the submarine proglacial area revealed several landforms identified as corresponding to an advance taking place between 1978 and 1985, although these forms are difficult to distinguish from annual winter push moraines (Grześ et al., 2009).

Jania et al. (2002) monitored the evolution of the flow velocity of Aavatsmarkbreen in the 1990s and 2000s. They compared velocities obtained from Global Positioning System (GPS) measurements of marked stakes in 2000 and 2001 to velocities derived using interferometry analysis of European Remote Sensing (ERS-1) Synthetic Aperture Radar (SAR) images acquired in March 1994 and April 1996. Summer velocities of the glacier terminus measured in July 2000 were between 0.091 and 0.136 m/day, while spring velocities in April 2001 ranged from 0.025 to 0.42 m/day. Jania et al. (2002) stated that the ground velocity data measured in the early 2000s were higher than the velocities derived in 1994 and 1996 but did not present data for the earlier period.

The thermal structure of the glacier was investigated in 1983 in a joint study by the Norwegian Polar Institute and the Scott Polar Research Institute (Bamber, 1989). Airborne radio echo soundings at 60 MHz revealed the presence of a prominent internal reflection horizon at a mean depth of 110 m, extending from the front to >13-km up-glacier, marking the separation between warm ice below and cold ice above. The bed reflector
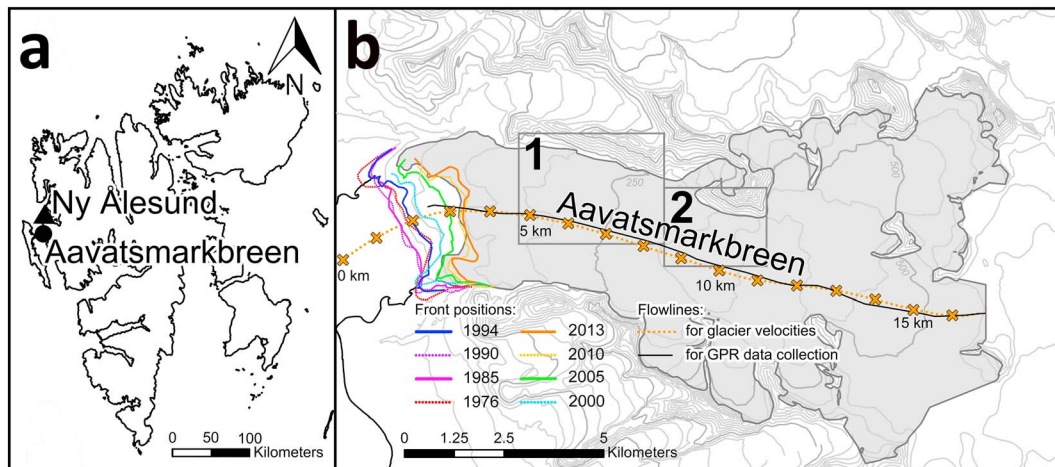
Figure 1. (a) Location of Aavatsmarkbreen (black dot) on the Norwegian archipelago of Svalbard and of the research station of Ny Ålesund (black triangle). (b) Topographic map of Aavatsmarkbreen, modified from http://toposvalbard.npolar.no (Norwegian Polar Institute), gray glacier outline is from September 2007, downloaded from the Randolph Glacier Inventory 5.0 (Pfeffer et al., 2014). The orange dotted line, marked every kilometer, represents the glacier centerline used to extract glacier velocities. The continuous black line marks the 2015 Ground Penetrating Radar (GPR) survey. Front positions were mapped from Landsat images (Table S1). Close-ups of zones a and b provided in Figure 7.

was obscured, but the transition between cold ice at the surface and warm ice below was clearly detected, showing that the glacier must have been entirely warm based at that time (Figure 2a).

Following its advance in the early 1980s, Aavatsmarkbreen underwent sustained recession. It retreated over 600 m between 1990 and 2000 (60 m/a) and lost another 700 m in length between 2000 and 2006 (116 m/a; Grześ et al., 2008; Lankauf, 1999). Increasing separation between successive retreat moraines on the seafloor indicates acceleration of the glacier retreat from 2001 to 2004 (Grześ et al., 2009). Recent estimates of the mass balance of the glaciers in this part of Svalbard between 2006 and 2010 are −0.57 m/a (Sobota, 2013), while elevation changes for NW Spitsbergen averaged around −0.54 ± 0.10 m/a between 2004 and 2008 (Moholdt et al., 2010).
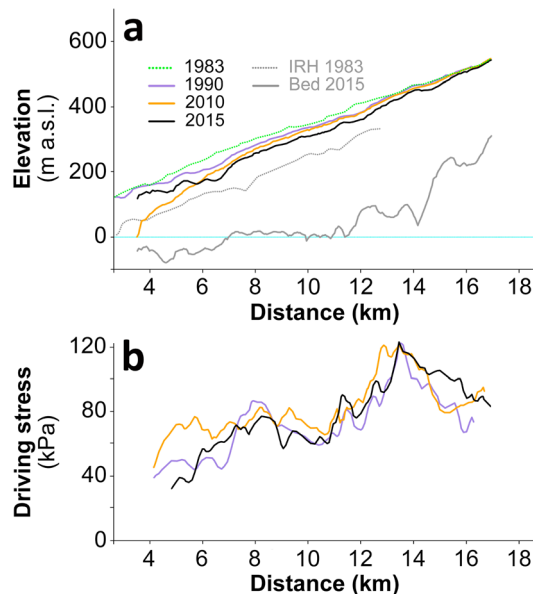

Figure 2. Evolution of the surface geometry and driving stress before and after the surge of Aavatsmarkbreen. (a) Surface profiles derived from Digital Elevation Models (Table S1) along the glacier centerline (orange dotted line in Figure 1). Bed topography and 2015 surface profile were measured in May 2015. Internal reflecting horizon (IRH) identified in 1983 from data collected by the Norwegian Polar Institute and the Scott Polar Research Institute (Bamber, 1987). (b) Driving stress calculated from equation (1).

2.2. Wahlenbergbreen

Wahlenbergbreen (78.55°N 13.90°E) is a 26-km-long tidewater glacier on the west side of Isfjorden, Oscar II Land, Svalbard (Figure 3). The glacier reaches a maximum elevation of 1,015 m a.s.l. (Nuth et al., 2013). The main trunk of the glacier flows from NW to SE and is confluent with a series of smaller tributaries from the SW. The lower part of the glacier is strongly constrained by topography and forms a 1.3-km wide calving front terminating in Yoldiabukta. It is not known whether Wahlenbergbreen sits on deformable sediments or a hard bed.

Before its most recent surge, Wahlenbergbreen last surged in 1910 (Liestøl, 1969). In 1908 the glacier extended almost to the mouth of Yoldiabukta, 6.6 km further out than its position in 1896 (De Geer, 1910; Hagen et al., 1993; Liestøl, 1969). The glacier surged a few years after its neighbor Sveabreen, and both glaciers eventually reached a maximum position in 1910 forming a common front (Figure 3). Subsequently, Wahlenbergbreen underwent calving retreat, interrupted by a still-stand from the 1980s to 2005 when the glacier terminus stabilized at a rock ridge projecting from the north side of the fjord, which acted as a pinning point.

Information on the thermal regime of Wahlenbergbreen was collected in 1983 by the Scott Polar Research Institute along a 10-km-long centerline profile starting from the glacier terminus
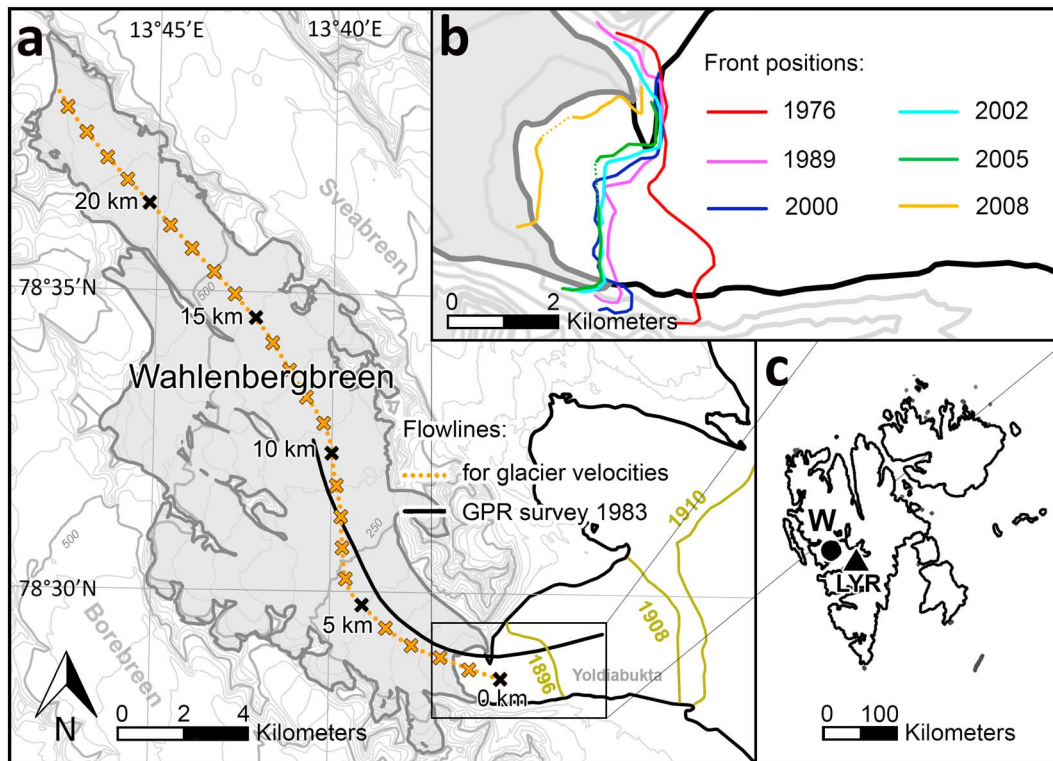
Figure 3. Location of Wahlenbergbreen in Svalbard. Topographic map modified from http://toposvalbard.npolar.no (Norwegian Polar Institute), gray glacier outline is from 2007, downloaded from the Randolph Glacier Inventory 5.0 (Pfeffer et al., 2014). Glacier front positions from 1976 to 2008 mapped using Landsat images (Table S1), older front positions from Hagen et al. (1993), Plassen et al. (2004), and De De Geer (1910). The orange dotted line, marked every kilometer, represents the glacier centerline used to extract glacier velocities. The continuous black line marks the 1983 GPR survey line (Bamber, 1987).

(Figure 4), using a radio echo sounder with a 60-MHz center frequency (Bamber, 1987). The data show a typical Svalbard-type polythermal structure with a warm layer beneath a cold surface layer up to 200 m thick (Sevestre & Benn, 2015). Unusually, the cold-temperate transition surface (CTS) emerges at the surface ~500 m from the calving front (Bamber, 1987). Little is known about the mass balance of Wahlenbergbreen, although measurements of thickness changes have been made on the neighboring glaciers: Sveabreen and Borebreen have respectively lost an average of 0.36 and 0.26 m/a water equivalent between 1966 and 2005 (Nuth et al., 2010).

3. Methods
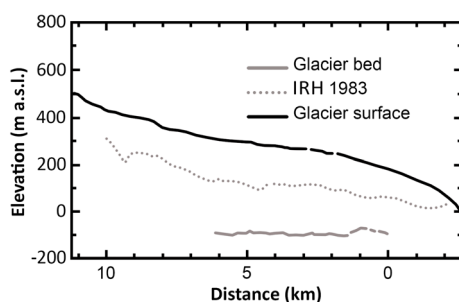
3.1. Remote Sensing

Figure 4. Interpretation of the centerline radargram collected in 1983 by Bamber (1987) on Wahlenbergbreen. For location see Figure 3. Modified from Bamber (1987).

Surface velocities of Aavatsmarkbreen and Wahlenbergbreen were derived using feature-tracking between sequential pairs of TerraSAR-X images acquired every 11 days, from December 2012 to October 2015 for Aavatsmarkbreen, and from September 2013 to October 2015 for Wahlenbergbreen. Surface features were tracked between pairs of images in slant range using a square correlation window of 200 pixels (~400 m) sampled every 20 pixels (~40 m) and subsequently orthorectified to a pixel size of 40 m using a Digital Elevation Model (DEM) based on aerial photographs from 1990 (Norwegian Polar Institute, 2014). Uncertainties in surface velocity arise from coregistration error (±0.2 pixels) and error arising from unavoidable smoothing of the velocity field over the feature-tracking window size. Using measured values of velocity from stationary features, we estimate the uncertainty to be better than 0.4 m/day. The presence of surface meltwater (or rain) decreases

backscatter and reduces coherence between images, reducing the quality of the image matches in the summer months, and we remove this noisy data from our analysis.

The evolution of surface crevasse fields on both glaciers was determined using TerraSAR-X backscatter images (a complete list of all satellite and aerial images used in this study is available in Table S1 in the supporting information). Crevasses were mapped manually using ArcGIS 10.3. Only crevasses larger than 2 m wide could be mapped, as the scenes have a spatial resolution of 2 m. Penetration of the radar signal in cold and dry snow is estimated to be up to 20 m (Rott & Nagler, 1994), although the presence of a small amount of water can reduce this number significantly. In addition snow may dampen the ability of crevasses to act like corner reflectors in the backscatter images. For this reason, the detection of small, narrow crevasses might be more challenging during the winter months. For this study, the upper limit of the crevasse field intersecting the centerline and the total crevassed area were measured on both glaciers. This measure enables us to monitor the changes in stresses affecting the glacier, while comparing the extent of the crevasse fields to the measured surface velocities along the centerline provides information on the connection between crevasses and glacier dynamics.

Additionally, the presurge evolution of the crevasse field of Aavatsmarkbreen was observed on aerial images from the Norwegian Polar Institute taken between July and August 2009, and on optical satellite images from DigitalGlobe (Google Earth) acquired on the 15 of July and 5 of August 2011. Three Advanced Spaceborne Thermal Emission and Reflection Radiometer (ASTER) scenes were used for similar purposes for Wahlenbergbreen between 2000 and 2009 (Table S1). Landsat images were also used to reconstruct front positions of the glaciers from 1976 to 2013 (Table S1). To quantify the uncertainty in mapping the front positions of the glaciers, we digitized a natural stationary feature found close to the glaciers (a mountain ridge) of the same length as the calving fronts, similarly to the method used by Moon and Joughin (2008). The offset between our mapping and the official map of the Norwegian Polar Institute was measured and averaged over the length of the shapefile (Table S2).

3.1.1. DEMs and uncertainties

A series of DEMs were used to measure changes in elevation of the glaciers prior to, during, and after the surge (see Table S1). ASTER DEMs were generated from original L1A stereo images using open-source software MicMac (Girod et al., 2016), which accounts and corrects for satellite shaking to resolve topography to greater than 10 m accuracy (Girod et al., 2017). In addition, Norwegian Polar Institute DEMs derived from vertical aerial photographs (Norwegian Polar Institute, 2014) and satellite DEMs from the SPOT-5 stereoscopic survey of Polar Ice: Reference Images and Topographies (SPIRIT) mission (Korona et al., 2009) are used for comparison. DEMs are differenced sequentially for both glaciers following coregistration and removal of satellite geometric biases (Nuth & Kääb, 2011). The resulting uncertainties are estimated from the surrounding (assumed stable) terrain with maximum standard deviations of 10 m. The Arctic DEM v2 was shifted by a constant value in the vertical using elevations from off-glacier points, extracted from mountain top elevations measured by the Norwegian Polar Institute. On average the difference in elevation between the Arctic DEM v2 and the map from the Norwegian Polar Institute was of 30.10 m over 17 points (Table S3).

3.2. Bed Topography of Aavatsmarkbreen

On the 8th of May 2015, 53 km of common-offset 5-MHz data were collected over Aavatsmarkbreen. The ground-penetrating radar was mounted on a wooden frame attached under a helicopter. Flying at ~40 km/hr gave a mean trace spacing of 30 m. The ice thickness was calculated assuming a constant wave velocity of 168×10^6 m/s. Due to inhomogeneities within the ice (primarily due to ice temperature), the wave velocity can vary within 2% (Navarro & Eisen, 2009), which gives an uncertainty of ±9 m in the depth calculations. The interpretation of the centerline bed topography and the surface profiles are displayed in Figure 2. More information on the radar system and data processing can be found in supporting information Text S4 (Lindbäck et al., 2014).

3.3. Driving Stress of Aavatsmarkbreen

Driving stresses were derived from the 2015 bed topography and centerline surface elevation profiles from 1990 to 2015 to fully bracket the presurge, surge, and postsurge conditions of Aavatsmarkbreen. The ice thickness was updated for each time period, and the surface slope was recalculated each time from the updated surface elevation profile. Although data on the bed topography of Wahlenbergbreen were

acquired by Bamber (1987) more than 30 years ago, the uncertainties in the data and in the positioning did not allow us to confidently calculate the changes in the driving stress of this glacier.

Driving stress τ_d is calculated from

$$\tau_d = \rho_i g h \tan\alpha \tag{1}$$

where ρ_i is the ice density, g gravity, h is ice thickness, and α the surface slope (Hooke, 2005).

The surface slope and driving stress were originally calculated over 150 m and subsequently averaged ever 1,600 m, or approximately 8 ice thicknesses, to smooth out the effect of longitudinal stress gradients. Bindschadler et al. (1977) recommended averaging between 8 and 16 times the ice thickness. We chose to adopt the bottom end of this range to avoid excessive data loss near the terminus. A greater averaging length would simply smooth out the data further, removing some of the peaks and troughs that we do not rely on for our analysis.

3.4. Weather Data

Two data sets of daily averaged air temperature and precipitation were downloaded from Eklima.no (Norwegian Meteorological Institute): first from the Ny Ålesund station (23 km north of Aavatsmarkbreen, at 8 m a.s.l. about 200 m from the ocean), from the 30th of December 2012 to the 30th of October 2015 (black triangle in Figure 1), and second from Longyearbyen airport (40 km south-east of Wahlenbergbreen, found at 28 m a.s.l. and 400 m from the ocean), from the 27th of September 2013 to the 26th of October 2015 (black triangle in Figure 3).

4. Results

4.1. Presurge Evolution of the Glaciers

4.1.1. Aavatsmarkbreen

Since the previous surge of the glacier in the early 1980s, Aavatsmarkbreen underwent rapid retreat combined with thinning of the terminus (Figures 1 and 2). The cumulative effect of the thinning was most pronounced over the lower part of the glacier. Between 1990 and 2010, the glacier lost 150 m in thickness (7.5 m/a) at the position of the 2010 front and about 50 m in thickness 2 km upstream (2.5 m/a). As a result, the surface slope of the lower part of the glacier steepened from 2.9° to 5.3° in only 20 years. Interestingly, no other significant changes in elevation could be detected higher up-glacier over the same period (Figure 2a). Inspection of Landsat images and of multiple DEMs did not reveal the presence of a surge bulge on the glacier prior to the surge, similar to the situation before the surges of tidewater glaciers Osbornebreen (Rolstad et al., 1997), Fridtjovbreen (Murray et al., Luckman, et al., 2003), and Monacobreen (Murray, Luckman, et al., 2003; Murray, Strozzi et al., 2003).

This rapid change in surface slope had a strong impact on the driving stress in the terminal zone (Figure 2b). In 1990, while the glacier was still in early quiescence after the 1980s surge, driving stresses on the lowermost 3 km of the glacier, where the bed is below sea level, were generally below 55 kPa, except above a bump on the bed (around kilometer 8 in Figure 2) where it reached 85 kPa. By 2010, the driving stress consistently increased over the previously low-stress regions, reaching values over 63 kPa over the lowermost 3 km, peaking at 76 kPa around kilometer 6.

While retreating and steepening, Aavatsmarkbreen was also steadily accelerating. The terminal crevasse field of the glacier can be seen expanding from 2000 to 2010, and from 2010 to 2013 (Figure 5). This spreading is confirmed on higher-resolution imagery in Figure 6 between 2009 and 2011. The formation of narrow (<1 m) extensional crevasses exposes the gradual stretching of the glacier terminus relative to the rest of the glacier. Another line of evidence confirms this acceleration: velocities measured by Jania et al. (2002) show an acceleration of the glacier between the mid-1990s and the early 2000s. Third, presurge velocities extracted from our TerraSAR-X data set at the glacier front reached 0.7 m/day by December 2012 (Figures 7 and 8), which shows an increase in velocities from those measured by Jania et al. (2002) in the early 2000s.

4.1.2. Wahlenbergbreen

Prior to its recent surge, Wahlenbergbreen retreated significantly from its 1910 extent. From 1910 to 1976 the glacier lost 6.8 km (103 m/a; Figure 3). The glacier lost another 600 m (43 m/a) before reaching a somewhat stable position in the late 1980s, supported by a prominent rock bar on the north side of the fjord. The glacier front only retreated past this pinning point in 2005 (Figure 3). In association with this retreat, the lower 7 km
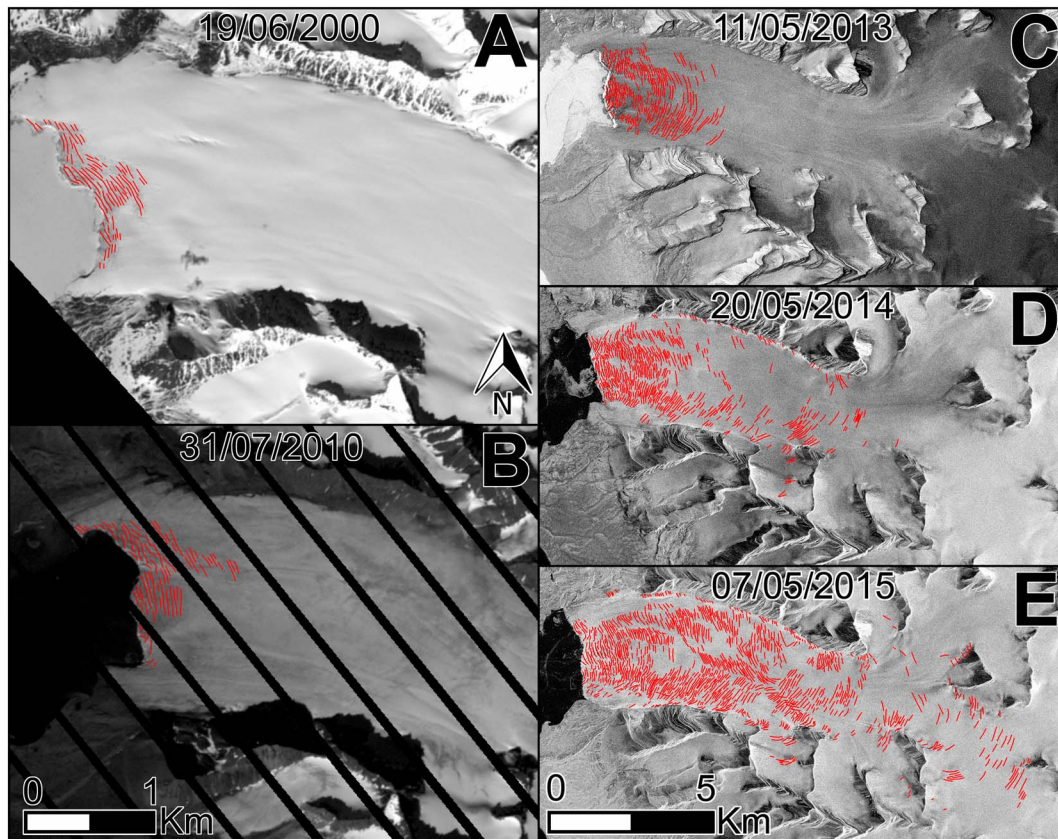
Figure 5. Evolution of the terminal crevasse field from 2000 to 2015 for Aavatsmarkbreen using Landsat (a and b), and TerraSAR-X scenes (c–e; Table S1). Individual crevasses are mapped in red.

of the glacier thinned and steepened between 2000 and 2009 (Figure 9). The thinning was most pronounced over the lower reaches of the glacier, with surface lowering of 52 m at the front, 38 m at kilometer 4 and on average 18 m over the next 6 km upstream, while a slight thickening could be detected farther up-glacier (Figure 9). These elevation changes resulted in a gradual steepening of the glacier, although more spatially spread out than on Aavatsmarkbreen. The slope over the lower 4 km of the glacier increased from 2.4° to 2.8° between 2000 and 2009.

The terminal crevasse field of Wahlenbergbreen expanded up-glacier in the years prior to surge onset (Figure 10). The total crevassed area more than doubled between 2000 and 2010 from 1.66 to 4.08 km^2. Extensional crevasse fields covered the lower 1.8 km of the glacier by 2010. The glacier front also advanced slightly between 2009 and 2010 (Figure 10).

4.2. Surge Initiation and Development
4.2.1. Aavatsmarkbreen

Surface velocities started to increase from presurge values of 0.5–0.6 m/day in May 2013, coinciding with the onset of positive air temperatures and the disappearance of sea ice in front of the glacier (Figures 7 and 8). Velocities rapidly increased over the lower 2 km of the glacier, reaching 2.1 m/day at the end of the melt season with a peak at 3.3 m/day at the terminus. Two kilometers further up-glacier, the velocities rose from 0.1 m/day to almost 1 m/day over the same period. Simultaneously, the upper limit of the crevasse field expanded from kilometers 6.2 to 9 (Figure 7). During the following winter, the average velocities between kilometers 4 and 5 slightly decreased (Figure 8). No sea ice could be observed from Landsat images in Hornbækbukta during this period. Velocities higher up-glacier remained the same throughout the winter and the spring. The crevasse field kept expanding up-glacier, reaching kilometer 12 by May 2014 (Figure 7).

A second step-change in velocities began in May 2014 at the onset of the melt season. The velocities between kilometers 4 and 5 doubled in 4 months, peaking at 4.5 m/day in mid-August 2014 (Figures 7 and 8). A core of
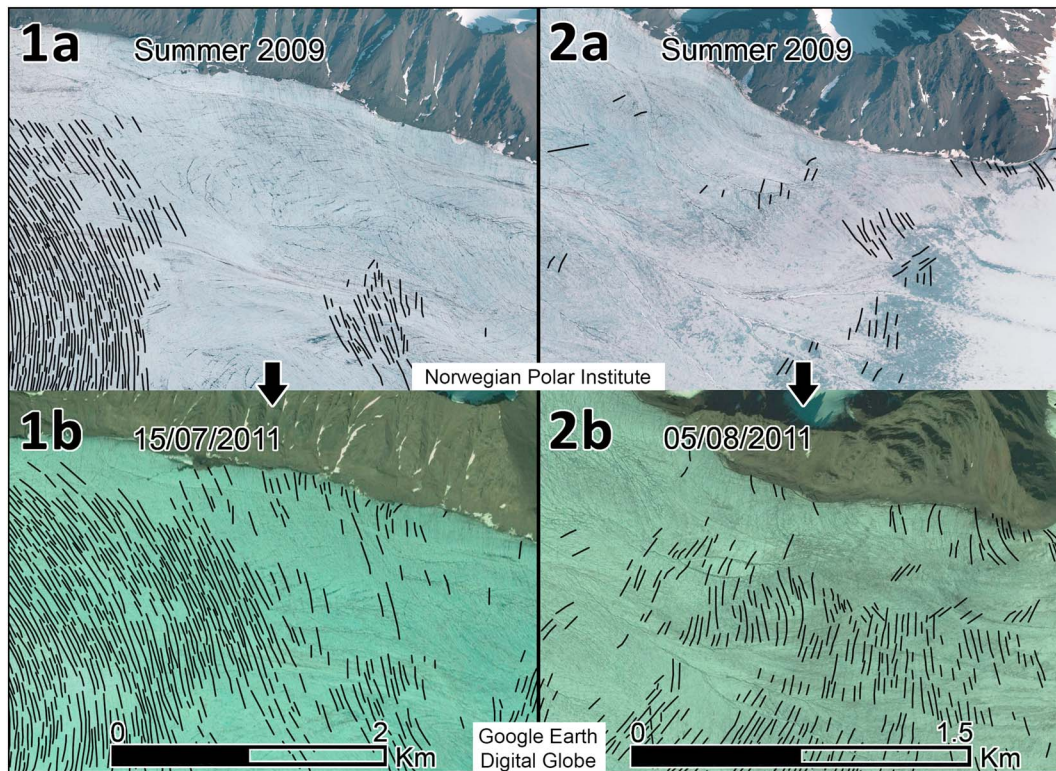
Figure 6. Comparison of surface crevassing between 2009 and 2011 for Aavatsmarkbreen. Images from 2009 are from the Norwegian Polar Institute (Toposvalbard. npolar.no), images from 2011 are from DigitalGlobe (Google Earth; Table S1). The contrast of the images was enhanced. See Figure 1 for the location of zones a and b.

very high velocities (>3.5 m/day) was recorded over the lower 1.5 km of the glacier (Figure 7). This velocity peak corresponded to a slight retreat of the glacier. Large velocity changes also occurred further up-glacier, in the region newly affected by extensional crevassing, and velocities more than doubled between kilometers 6 and 10. Strong velocity gradients can be observed along the glacier margins. Throughout the surge, a region of consistently lower velocity occurred ~3.5 km from the front, which corresponds to a bedrock bump and zone of high driving stresses shown in Figures 2 and 7. The uppermost position of the crevasse field was located at kilometer 14 at the end of September 2014. The crevasses were almost exclusively transverse to ice flow, reflecting longitudinal extension (Figures 5d and 5e).
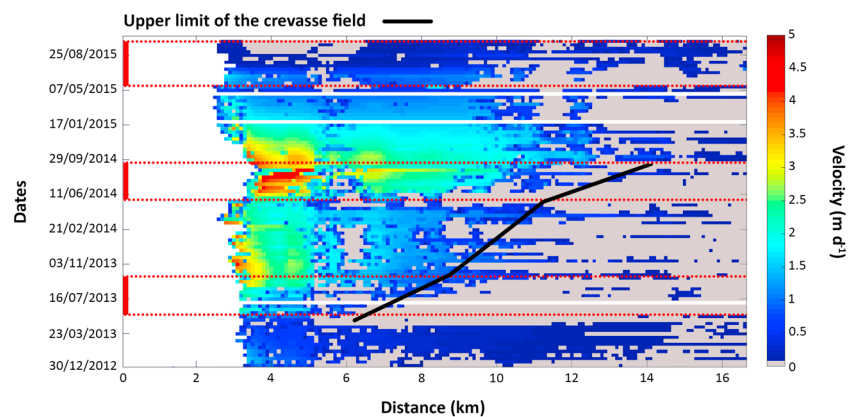

Figure 7. Time series of the velocities measured along the centerline profile of Aavatsmarkbreen from feature-tracking between pairs of TerraSAR-X images. The glacier flows from right to left. Melt seasons are bracketed by the red dotted lines. The thick solid black line represents the position of the upper limit of the crevasse field, intersecting the glacier centerline, and mapped using TerraSAR-X images (Table S1).
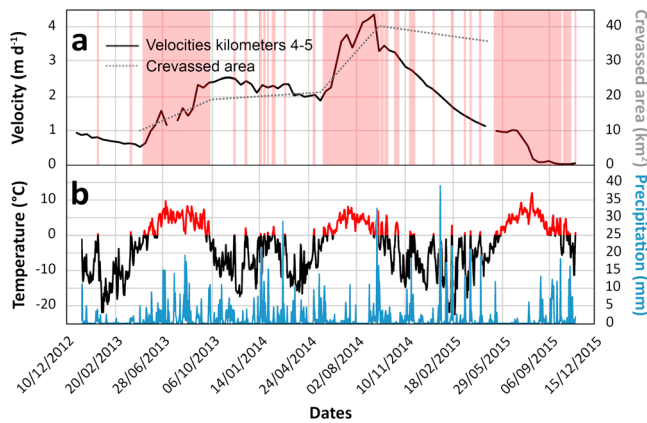
Figure 8. (a) Velocities of Aavatsmarkbreen glacier throughout its surge averaged between kilometers 4 and 5 (Figure 1 for kilometers). The gray dotted line represents the total crevassed area on the glacier measured using TerraSAR-X images. Melt seasons are shaded in red. (b) Daily air temperature (in red and black) and precipitation (blue) collected at Ny Ålesund (from eklima.no, Norwegian Met Office), for location see black triangle in Figure 1a.

4.2.2. Wahlenbergbreen

Wahlenbergbreen started to advance between August 2009 and August 2010 (Figures 10b and 10c). The velocities of Wahlenbergbreen were already on the rise when our acquisitions began in autumn 2013 (Figures 11 and 12). During the winter of 2013–2014, flow speeds on the lower glacier remained just over 1 m/day, while a small increase was detected higher up-glacier between kilometers 6 and 7 reaching 0.6 m/day (Figure 12a). Further up-glacier, velocities remained below 0.3 m/day (Figure 11). The upper limit of the crevasse field remained at kilometer 8.5 throughout the winter (Figure 11).

A strong but short-lived velocity increase was detected during the next melt season between May and August 2014. Velocities peaked at 1.93 m/day at the front and at 0.85 m/day between kilometers 6 and 7 and fell back to 1.4 and 0.5 m/day respectively by August. The upper limit of the crevasse field shifted slightly further up-glacier reaching kilometer 9.2 (Figure 11). Following the end of the melt season, velocities increased steadily, and by the end of winter 2014–2015 the lower 9 kilometers of the glacier were flowing above 1.5 m/day. The apparent reduction in the extent of the crevasse field during the winter is likely due to snow cover on the TerraSAR-X scene, obscuring smaller crevasses at the upper end of the field.

The onset of the 2015 melt season corresponded with a large step-change in velocity affecting the glacier up to kilometer 14. Velocities between kilometers 1 and 2 peaked just under 5 m/day, while velocities between
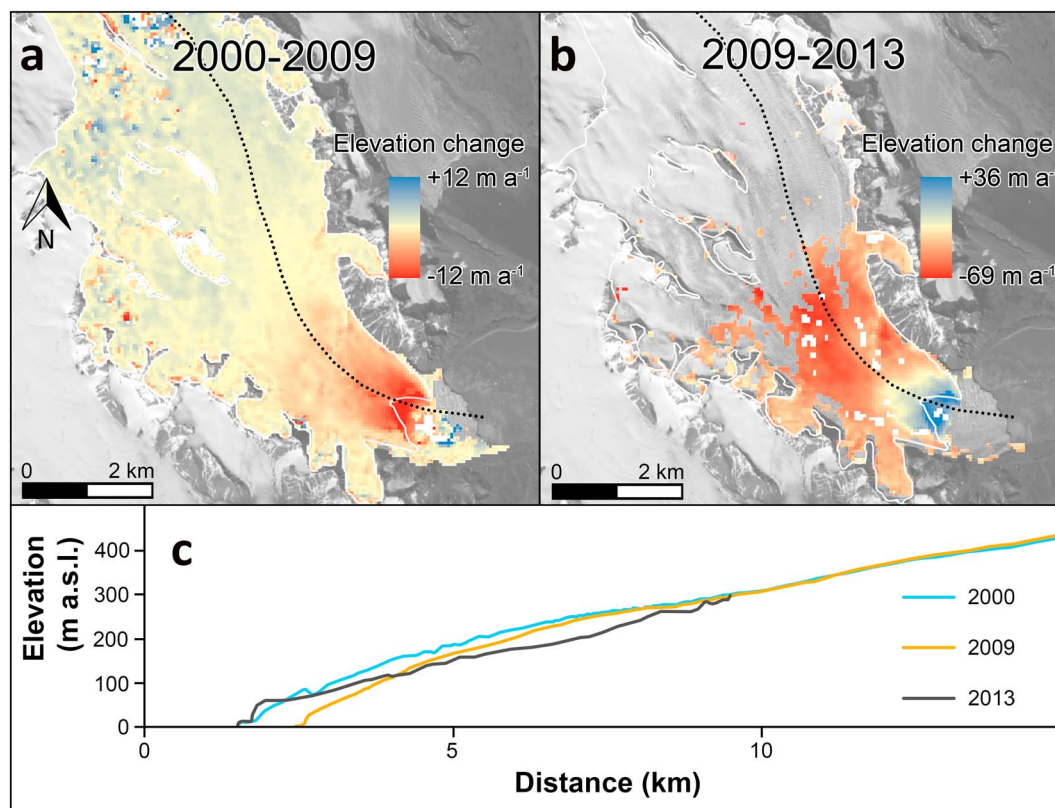
Figure 9. Changes in surface elevation of Wahlenbergbreen prior to and during the most recent surge (2014). (a) Digital Elevation Model differencing between 2000 and 2009, (b) Digital Elevation Model differencing between 2009 and 2013. Background image is a Landsat 8 collected on the 9 of July 2016. Please note the change in color scale between a and b. (c) Elevation profiles along the glacier centerline (black dotted line) in 2000, 2009, and 2013. Outlines from September 2007, from the Randolph Glacier Inventory 5.0.

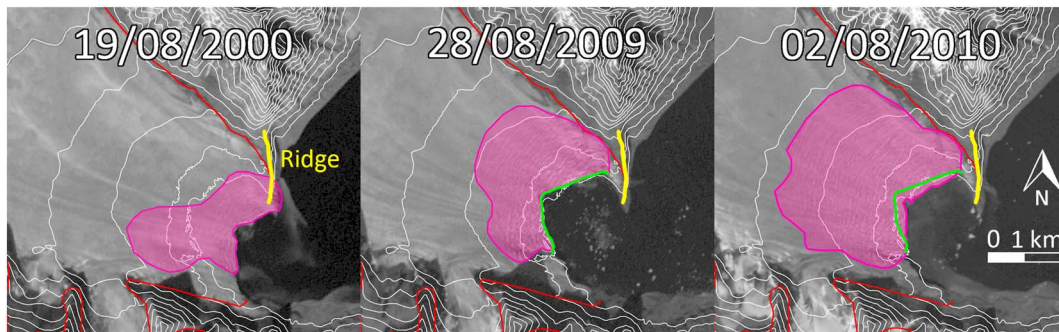**Figure 10.** Evolution of the terminal crevasse field of Wahlenbergbreen, mapped using ASTER images (Table S1). The green line delineates the 2009 glacier front.

kilometers 6 and 7 reached 3.7 m/day at the same time. The upper limit of the crevasse field dramatically migrated further upstream, and the lower 24 km of the glacier was covered by extensional crevasses by the end of October 2015. Regions between kilometers 9 and 14, which were unaffected by the surge the previous summer, accelerated from 1 to 3 m/day. The gradual decrease in temperatures did not slow the glacier down, and by the end of our acquisition period, the velocities between kilometers 6 and 7 were approaching 5 m/day. Due to the high velocities and the chaotically broken-up glacier surface at the terminus, the feature-tracking algorithm could not efficiently track the lower portions of the glacier during this phase of the surge. Our acquisitions of TerraSAR-X scenes for Wahlenbergbreen ended on the 26 of October 2015 while the surge continued.

The surge drastically affected the geometry of the glacier. Between 2009 and 2013, the glacier advanced over 1 km and thickened over the lower 1.5 km, gaining 58 m at the location of the 2013 glacier front, while between kilometers 4 and 9.5 a large drawdown was detected, with up to 42 m of surface lowering in places. The surface profile of the glacier flattened to an average of 1.7° over the lower 4.5 km.

4.3. Termination of the Surge of Aavatsmarkbreen

The peak in velocities in summer 2014 was followed by a steady decrease in velocities (Figures 7 and 8). The precipitation total from August to November 2014 was double that of the same period in 2013 (Figure 8). In addition, periods of positive air temperatures occurred throughout October and early November 2014 —unlike the previous year—and much of this precipitation likely fell as rain. From February to May 2015 glacier velocities over the lower 7 km of the glacier declined steadily, and by June 2015 had reached 0.8 m/day (Figures 7 and 8). A major slowdown of the whole glacier occurred between July and August 2015, and velocities over the lower 7 km of the glacier went from 0.7 m/day to presurge values of 0.1 m/day.

The 2-year-long surge significantly changed the geometry of Aavatsmarkbreen. The glacier advanced over 1 km between May 2013 and May 2015, although it did not reach its previous maximum surge extent. A clear

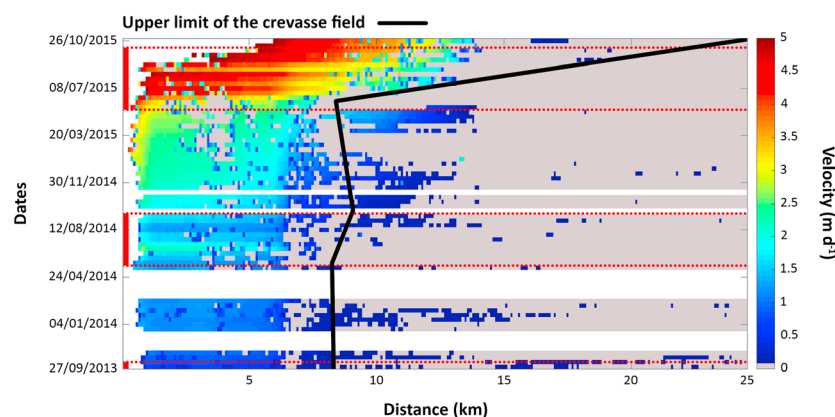**Figure 11.** Time series of the velocities measured along the centerline profile of Wahlenbergbreen from feature tracking between pairs of TerraSAR-X images (Table S1). The glacier flows from right to left. Melt seasons are bracketed by the red dotted lines. The thick solid black line represents the position of the upper limit of the crevasse field, intersecting the glacier centerline, and mapped using TerraSAR-X images.
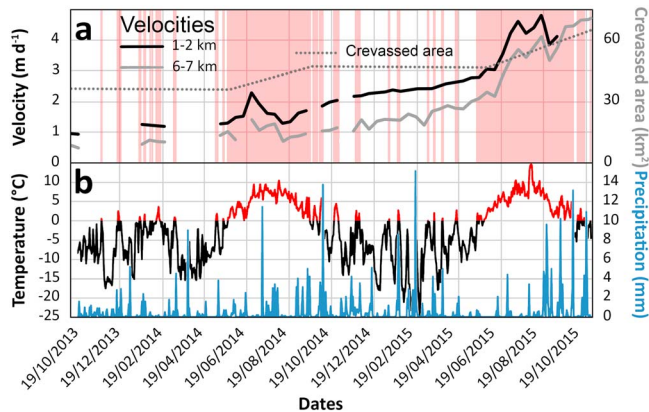
Figure 12. (a) Velocities of the glacier Wahlenbergbreen from feature tracking between pairs of TerraSAR-X images (Table S1). The gray dotted line represents the total crevassed area on the glacier measured using TerraSAR-X images. Melt seasons are shaded in red. (b) Daily air temperature (in red and black) and precipitation (blue) collected at Longyearbyen airport (from eklima.no, Norwegian Met Office). For location see black triangle in Figure 3.

drawdown of the glacier surface is evident from the postsurge DEM (Figure 2a). An average of 13 m in thickness were lost between kilometers 4 and 14.3 between 2010 and 2015. The overall slope of the 2015 profile is very similar to that of 1990, except that the lowermost 4 km has a more irregular surface. This was clearly observed in the field during the 2015 GPR survey. After the surge, the driving stress rapidly dropped below presurge levels, reaching its lowest values in 25 years at the glacier front from kilometers 4.8 to 6 and 7.5 to 9.

5. Summary

The evolution of the glaciers prior and during their surges can be summarized as follows.

1. Both glaciers underwent significant retreat in the decades before surging. Wahlenbergbreen lost 1.5 km in length between 1976 and 2010, and Aavatsmarkbreen retreated over 1.7 km between 1983 and 2013. In addition to retreating, both glaciers thinned and steepened. On Aavatsmarkbreen, the surface slope rose from 2.9° to 5.3° over the lower 4 km. As a result, driving stresses over the terminal zone of the glacier increased, especially in areas characterized by very low values in the early quiescence phase. On Wahlenbergbreen the steepening was more spread out over the lower 9 km. Evolution of the driving stress could not be calculated on this glacier, but an overall increase can be inferred from geometrical changes between 2000 and 2009.

2. During the same period, flow velocities of Aavatsmarkbreen underwent a slow increase, rising from 0.1 to 0.15 m/day in the early 2000s to 0.5–0.6 m/day in late 2012. This long and gradual buildup on a retreating glacier was also observed on Basin 3, Austfonna, by McMillan et al. (2014).

3. No thickening of the upper part of Aavatsmarkbreen occurred during the quiescent period, while a minor thickening (~1 m/a) was detected in the upper reaches of Wahlenbergbreen.

4. Both glaciers experienced expansion of their terminal crevasse fields in the decade before surging. The crevasses are predominantly perpendicular to flow, indicative of extension.

5. For both glaciers, the transition to fast flow occurred in the space of a few weeks and coincided with the onset of positive air temperatures. Velocities at the front of Aavatsmarkbreen doubled during the 2013 melt season, while the lower 7 km of Wahlenbergbreen almost doubled in speed between June and August 2014. This led directly to the up-glacier migration of the region of extensional crevasses.

6. During the following autumn and winter, the velocities of Aavatsmarkbreen declined slightly, while Wahlenbergbreen kept on accelerating steadily after a postsummer drop in velocities.

7. Velocities of both glaciers significantly rose again the following melt season, with Aavatsmarkbreen doubling in speed by August 2014 compared to the previous summer, reaching 4.5 m/day at the front, and the terminus of Wahlenbergbreen going from 2.3 m/day in June 2014 to 4.85 m/day in August 2015. Subsequently, the crevasse fields of both glaciers rapidly expanded further up-glacier. High velocities were detected higher up than the previous summer on both glaciers, and new regions became mobilized into the surges.

8. At the end of the second melt season, Wahlenbergbreen continued surging, but our acquisitions for this glacier ended. More recent SAR data from Sentinel-1 (not analyzed here) indicate that Wahlenbergbreen continued to surge into 2017 and beyond. Aavatsmarkbreen began a steady decline in velocities throughout the winter of 2014–2015. The 2015 melt season reactivated fast flow for a few weeks, but eventually velocities plummeted between July and August 2015, returning to levels recorded in the early 2000s.

9. Large drawdown of the longitudinal elevation profile of Aavatsmarkbreen occurred between 2010 and 2016, with a more extended front position and on average a lower surface gradient over the lower 4 km of the glacier. Driving stresses fell below the presurge values over the portions of the glacier. The centerline elevation profile of Wahlenbergbreen bore similarities to that of Aavatsmarkbreen with a strong thickening of the lower 4 km and a drawdown further up.

6. Discussion

For Aavatsmarkbreen, for which more complete data are available, the sequence of events indicates a two-stage process of surge initiation. The first stage, from ~1990 to 2012, consisted of a gradual increase in velocity associated with steepening of the glacier terminus and significant increase in driving stress. In spite of the thinning of the terminus, we have grounds to believe that the glacier still had temperate ice all the way to the calving front. Thinning polythermal Arctic and subarctic glaciers have been observed to progressively lose their zone of temperate ice in response to the deeper penetration of the winter cold wave (Rippin et al., 2011; Wilson et al., 2013). However, this is a slow process, which can be offset by the advection of temperate ice from up-glacier. Modeling by Pettersson et al. (2007) estimated the recent downward migration of the CTS on Storglaciaren, northern Sweden, to be slower than 1 m/a, and it is likely to have been even slower on Aavatsmarkbreen, where mean annual air temperature is lower. To turn the base of Aavatsmarkbreen cold at the terminus, the CTS would have had to migrate vertically over 85 m in 30 years (1983–2013), which is highly unlikely. We therefore believe that the deepest portions of the terminus of Aavatsmarkbreen were still temperate before the surge.

The driving stress was able to rise because the change in surface slope α was proportionally greater than the decrease in glacier thickness h (equation (1)). Between 1990 and 2010 the gradient of the lower glacier almost doubled while the mean thickness decreased by only 24%. Increasing driving stress would, in turn, increase strain rates in the basal ice. According to Glen's flow law (Glen, 1955):

$$\dot{\varepsilon} = A\tau_d{}^n \tag{2}$$

where $\dot{\varepsilon}$ is strain rate, A the rate factor, and the exponent $n = 3$. An increase in both driving stress and strain rate would have resulted in an increase in melting of the temperate ice at and above the glacier bed (van der Veen, 2017):

$$\dot{M} = \frac{\tau_d\dot{\varepsilon}}{\rho_i L} \tag{3}$$

where $\dot{M}$ is melt rate, and L is the latent heat of melting. Thus, the observed 1.4-fold increase in shear stress (from ~50 to ~70 kPA) in the lower 3 km of the glacier would result in a 2.7-fold increase in strain rate, due to the cubic dependence of strain on stress, and a 3.8-fold increase in basal melt rate. Due to the impact of water on both sliding rates and the softness of glacier ice, increased melting will have encouraged further acceleration of the glacier, particularly if the basal drainage system was undeveloped and inefficient. This process may have led to a positive feedback between velocities and strain heating and could have eventually led to a surge after a long buildup. However, the sudden increase in velocity at the beginning of the 2013 melt season and a second step change in velocities the following summer indicate that other factors determined the character of the main surge event.

The second stage of the surge extended from early summer 2013 to spring 2015, with two rapid speedups coincident with the onset of positive air temperatures in the 2013 and 2014 melt seasons. Although the first speedup was also synchronous with the breakup of sea ice in front of the glacier, sea ice was not present in winter 2013–2014. Similarly, sea ice was also absent during the years leading to the surge of Wahlenbergbreen. Loss of sea ice can therefore be discounted as a possible trigger for rapid motion. We attribute both speedups to the routing of surface meltwater to the glacier bed via crevasses, reducing bed strength and increasing rates of basal motion. The changing spatial extent of surface crevasses is consistent with this hypothesis. Narrow crevasses appeared on the surface of Aavatsmarkbreen between 2009 and 2011, reflecting the slow and gradual increase in velocity during stage 1. Large extensional crevasses were only present in the lower 1.7 km of the glacier in 2011 but had propagated 4.5 km up-glacier by the end of 2012. The extent of these crevasses coincided with the area most affected by 2013 speedup (Figure 7). Velocities continued to increase throughout the melt season and then dropped slightly during the following winter. This suggests constant or slightly diminishing water storage at the bed. Over the winter months, crevasses continued to propagate up-glacier as the geometry adjusted to fast flow on the lower tongue, and by January 2014 reached 400 m a.s.l. 8 km up-glacier from the terminus. With the onset of melting in 2014, glacier velocities again increased rapidly, affecting a much larger portion of the glacier. The expansion of the crevasse field meant that greater volumes of meltwater could efficiently reach the bed, mobilizing a greater area of the glacier.

Aavatsmarkbreen underwent steady deceleration shortly after the velocity peak of August 2014. The deceleration lasted much longer than the short acceleration phases, as also occurred on Monacobreen (Murray, Strozzi, et al., 2003). This is unlike the rapid termination of the 1982–1983 surge of Variegated Glacier, Alaska, attributed by Kamb (1987) to the formation of an efficient channelized subglacial drainage system. Rather, the gradual deceleration phase suggests more gradual leakage of water from beneath the glacier over the winter months. Although large extensional crevasses covered the whole glacier surface in summer 2015, presumably enabling surface-to-bed drainage to occur once again, there was only a minor, short-lived velocity peak at that time. This implies that an efficient drainage system developed rapidly after the onset of surface melt, resulting in a sharp decrease in velocities between July and August 2015.

Although we have less comprehensive data for Wahlenbergbreen, the observations are consistent with similar surge mechanisms on that glacier. As was the case for Aavatsmarkbreen, the surge was preceded by an up-glacier expansion of the terminal crevasse field. This could be the result of the gradual steepening of the glacier and a possible increase in driving stress, although it could also be related to calving retreat from the pinning point after 2005 (Figure 3). Ice-margin retreat from the major topographic barrier presented by the rock ridge will have caused a significant reduction in backstress on the glacier front, encouraging extension of the terminal zone. The start of the surge coincided with the onset of the 2014 melt season and only affected ice within the terminal crevasse field (Figure 11). The second acceleration followed melt onset in 2015, after which the area of fast-flowing ice expanded rapidly up-glacier, lagging the migration of the upper limit of the crevasse field. We conclude that the switch to fast flow occurred when surface meltwater was able to access the bed via crevasses.

Thus, we argue that the surges of both glaciers were preconditioned by the formation of crevasse fields on their lower tongues. Once formed, the crevasses allowed penetration of surface meltwater to the bed, and the resulting flow acceleration caused extensional flow and crevasse formation up-glacier, which in turn caused up-glacier propagation of the region of fast flow. The causes of initial crevasse-field formation may have been different on the two glaciers. On Aavatsmarkbreen, ablation-driven steepening of the glacier tongue appears to have triggered a stress strain heating feedback and gradual acceleration, whereas on Wahlenbergbreen, glacier steepening combined with retreat from a pinning point likely played an important role. The loss of pinning points on retreating marine terminating glaciers has been shown to increase extension and enhance further retreat (McNabb & Hock, 2014; O'Neel et al., 2005). In the particular case of Wahlenbergbreen, the loss of the backstress formerly provided by the rock bar resulted in stretching and crevassing of the lower part of the glacier, although this did not directly lead to a surge. Additional and specific circumstances were required to tip the glacier into a full-blown surge.

It has now been widely demonstrated that inputs of glacial meltwater to the subglacial environment are directly related to changes in ice dynamics and more particularly rates of basal motion. Studies have shown that terrestrial and marine terminating outlets of the Greenland ice sheet can speed up in response to increased meltwater inputs (Andersen et al., 2010; Bartholomew et al., 2011; Palmer et al., 2011; Sole et al., 2011; Zwally et al., 2002), as well as the drainage of supraglacial lakes (Das et al., 2008).

In the case of surges that initiate in a reservoir zone on the upper part of a glacier, feedbacks between flow speed and strain heating are sustained by increasing driving stress during mass accumulation and glacier thickening. In contrast, the velocity-strain heating feedback we infer on Aavatsmarkbreen occurred in an area of mass loss and thinning. In this case, driving stresses were able to rise because the surface gradient increased at a greater proportional rate than that of thickness decrease. This relationship between changes in gradient and thickness is much less likely to occur at terrestrial glacier fronts, where thickness tends to zero, than on tidewater glaciers where thicknesses can remain large at the terminus.

On Wahlenbergbreen, initial expansion of the terminal crevasse field may have been caused by a combination of two factors: gradual steepening causing internal thermodynamic processes and glacier retreat from a pinning point. However, after the initial trigger, evolution of the surge was similar to that of Aavatsmarkbreen. This implies that surges might be internally or externally triggered or occur as the result of a combination of the two. This is consistent with the conclusions of other authors, who note that the distinction between surges and externally forced processes may not be straightforward (McMillan et al., 2014; Sevestre & Benn, 2015).

Surface meltwater routing via crevasses can be expected to lead to distributed storage at glacier beds, due to water influx at multiple, closely spaced recharge points. In turn, multiple recharge points and distributed storage will encourage low hydraulic gradients and water retention within the system, especially if the glacier lacks an extensive preexisting basal channel network. This process should therefore be a powerful mechanism for initiating or amplifying surges on glaciers with newly developing crevasse fields. Indeed, it appears to have played an important role in the evolution of a number of documented surges. The 1982–1983 surge of Variegated Glacier was preceded by a slow increase in velocities, with a switch to high speeds coincident with the onset of melt (Kamb et al., 1985). Similarly, multiple annual speedups were observed during the surge of Basin 3 of the icecap Austfonna in Nordaustlandet, Svalbard, by Dunse et al. (2015) and attributed to routing of surface meltwater to the bed via crevasses. This suggests that the evolution of many surges may be determined by two distinct processes, a first slow phase during which crevasse fields develop and a subsequent rapid phase triggered by surface-to-bed drainage.

Sevestre and Benn (2015) argued that it may be possible to explain all surges within a single conceptual framework, based on the enthalpy balance of the glacier. Enthalpy is a measure of the internal energy of a glacier, a function of its temperature and water content (Aschwanden et al., 2012). For warm-based polythermal glaciers such as Aavatsmarkbreen and Wahlenbergbreen to remain in steady state, they must flow at their balance velocities, and enthalpy gains from gravitational energy expenditure during ice flow must balance enthalpy losses in the form of runoff and heat conduction. The enthalpy cycle model relates surging to imbalances between enthalpy production and dissipation, and in the case of warm-based glaciers, cycles of meltwater production and evacuation (Sevestre & Benn, 2015). On land-terminating surge-type glaciers, enthalpy can increase below reservoir zones if feedbacks between flow speed and strain heating are sustained by increasing driving stress during mass accumulation and glacier thickening. In contrast, we infer an increase in enthalpy below the terminus of Aavatsmarkbreen in response to glacier steepening during retreat.

Routing of meltwater to the glacier bed can also be viewed as an enthalpy transfer process, because it increases the water storage (and hence enthalpy) of the basal zone. On cold glaciers, enthalpy transfer may take the form of refreezing of surface water (cryohydrologic warming) and may also be implicated in surge evolution (Dunse et al., 2015). Up-glacier propagating surges of tidewater glaciers, therefore, have both similarities and differences with the better known "downward-propagating" surges of land-terminating glaciers. Both can be understood in terms of enthalpy balance and reflect the interplay between regional (climatic) and local (geometry and subglacial topography) controls on glacier dynamics.

7. Conclusions

The upward-propagating surges of tidewater glaciers Aavatsmarkbreen and Wahlenbergbreen can be subdivided into slow and fast phases, distinguished by different processes impacting on modes of ice motion. During quiescence, both glaciers were retreating and thinning at their front. Steepening of the lower few kilometers of Aavatsmarkbreen resulted in an increase in driving stress, which likely enhanced strain heating and increased meltwater production. Feedbacks between strain heating and velocity initiated a gradual acceleration of the glacier and up-glacier expansion of the terminal crevasse field. Wahlenbergbreen also showed signs of a gradual acceleration, which could be linked to the steepening detected between 2000 and 2009 and to the loss of a pinning point (rock bar) at the front of the glacier.

The fast phase of both surges was triggered at the onset of the melt season; Aavatsmarkbreen and Wahlenbergbreen doubled in speed in the early summers of 2013 and 2014, respectively. The spatial extent of the speedup coincided with that of crevasse fields, showing that these significant step changes in velocity were triggered by routing of surface meltwater to the bed. During the following winter, the velocities of Aavatsmarkbreen gradually decreased suggesting water leakage from the bed, while Wahlenbergbreen continued to accelerate. Velocities doubled again at the onset of the second melt season, mobilizing greater areas of the glaciers and coinciding with continued expansion of their crevasse fields. By 2015 velocities on Aavatsmarkbreen gradually returned to presurge values. Wahlenbergbreen was observed to still be surging in 2017.

Downward-propagating surges occur following ice buildup in a reservoir zone during the quiescent period. In contrast, the two upward-propagating surges investigated in this study occurred after glacier retreating and thinning. We argue that the common factor is an increase in driving stress due to geometric changes during

quiescence, which sets in train a positive feedback between strain heating and ice velocity. Increases in driving stress during thinning are much more likely to occur on tidewater glaciers than land-terminating glaciers, because ice thickness can remain large at the front. Similarly, development of surface crevasse fields is implicated in the transition to rapid ice motion on both upward- and downward-propagating surges. All of these processes can be understood within the context of the enthalpy cycle model proposed by Sevestre and Benn (2015), which attributes surging to an imbalance between rates of enthalpy production and dissipation. Such imbalances may reflect both regional (climatic) and local (geometric and geological) factors.

Climate change is likely to impact surging behavior in different ways. Sevestre et al. (2015) argued that surges of small, land-terminating glaciers in Svalbard became less common through the twentieth century because of ice thinning and loss of accumulation zones. In contrast, surges of tidewater glaciers may become more common during ice thinning, if this results in increasing driving stresses. Additionally, rising rates of surface melt may also encourage instabilities on larger, crevassed glaciers (Dunse et al., 2015). As the effects of climate change bite deeper into the Arctic cryosphere, more wide-reaching changes in glacier dynamics may be expected.

Author Contribution

H. S., D. B., and A. L. designed the study. H. S. analyzed the velocities using data provided by A. L. and made the crevasse maps. H. S. drafted the manuscript with contributions from D. B. and A. L. D. B. calculated the stresses and edited the manuscript. C. N. extracted surface elevation profiles from the DEMS. J. K. K. L., K. L. collected the radio echo data acquired with an instrument built by R. P. and J. K. K. L. and R. P. processed the radar data.

References

Andersen, M. L., Larsen, T. B., Nettles, M., Elosegui, P., van As, D., Hamilton, G. S., et al. (2010). Spatial and temporal melt variability at Helheim Glacier, East Greenland, and its effect on ice dynamics. *Journal of Geophysical Research*, 115, F04041. https://doi.org/10.1029/2010JF001760

Aschwanden, A., Bueler, E., Khroulev, C., & Blatter, H. (2012). An enthalpy formulation for glaciers and ice sheets. *Journal of Glaciology*, 58(209), 441–457. https://doi.org/10.3189/2012JoG11J088

Bamber, J. L. (1987). Internal reflecting horizons in Spitsbergen glaciers. *Annals of Glaciology*, 9, 5–10. https://doi.org/10.1017/S0260305500000306

Bamber, J. L. (1989). Ice/bed interface and englacial properties of Svalbard ice masses deduced from airborne radio echo-sounding data. *Journal of Glaciology*, 35(119), 30–37. https://doi.org/10.3189/002214389793701392

Bartholomew, I. D., Nienow, P., Sole, A., Mair, D., Cowton, T., King, M. A., & Palmer, S. (2011). Seasonal variations in Greenland Ice Sheet motion: Inland extent and behaviour at higher elevations. *Earth and Planetary Science Letters*, 307(3–4), 271–278. https://doi.org/10.1016/j.epsl.2011.04.014

Bindschadler, R., Harrison, W. D., Raymond, C. F., & Crosson, R. (1977). Geometry and dynamics of a surge-type glacier. *Journal of Glaciology*, 18(79), 181–194. https://doi.org/10.1017/S0022143000021298

Clarke, G. K. C., Collins, S. G., & Thompson, D. E. (1984). Flow, thermal structure, and subglacial conditions of a surge-type glacier. *Canadian Journal of Earth Sciences*, 21(2), 232–240. https://doi.org/10.1139/e84-024

Das, S., Joughin, I., Behn, M. D., Howat, I. M., King, M. A., Lizarralde, D., & Bhatia, M. P. (2008). Fracture propagation to the base of the Greenland ice sheet during supraglacial lake drainage. *Science*, 320(5877), 778–781. https://doi.org/10.1126/science.1153360

De Geer, G. (1910). Guide de l'excursion au Spitzberg. Paper presented at the XIe Congrès Géologique International, Stockholm.

Dowdeswell, J. A., & Benham, T. J. (2003). A surge of Perseibreen, Svalbard, examined using aerial photography and ASTER high resolution satellite imagery. *Polar Research*, 22(2), 373–383. https://doi.org/10.3402/polar.v22i2.6466

Dunse, T., Schellenberger, T., Hagen, J. O., Kääb, A., Schuler, T. V., & Reijmer, C. H. (2015). Glacier-surge mechanisms promoted by a hydro-thermodynamic feedback to summer melt. *The Cryosphere*, 9(1), 197–215. https://doi.org/10.5194/tc-9-197-2015

Flink, A. E., Noormets, R., Kirchner, N., Benn, D. I., Luckman, A., & Lovell, H. (2015). The evolution of a submarine landform record following recent and multiple surges of Tunabreen glacier, Svalbard. *Quaternary Science Reviews*, 108, 37–50. https://doi.org/10.1016/j.quascirev.2014.11.006

Frappé-Sénéclauze, T. P., & Clarke, G. K. C. (2007). Slow surge of Trapridge glacier, Yukon Territory, Canada. *Journal of Geophysical Research*, 112, F03S32. https://doi.org/10.1029/2006JF000607

Girod, L., Nuth, C., Kääb, A., McNabb, R., & Galland, O. (2017). MMASTER: Improved ASTER DEMs for elevation change monitoring. *Remote Sensing*, 9(7). https://doi.org/10.3390/rs9070704

Girod, L., Ramuntcho, M., Nuth, C., & Kääb, A. (2016). Glacier volume change estimation using time series of improved ASTER DEMs. International Archives of Photogrammetry. *Remote Sensing and Spatial Information Sciences*, XLI-B8(B8), 489–494. https://doi.org/10.5194/isprsarchives-XLI-B8-489-2016

Glen, J. W. (1955). The creep of polycrystalline ice. *Proceedings of the Royal Society of London. Series A: Mathematical and Physical Sciences*, 228(1175), 519–538. https://doi.org/10.1098/rspa.1955.0066

Grześ, M., Król, M., & Sobota, I. (2008). *Glacier geometry change in the Forlandsundet area (NW Spitsbergen) using remote sensing data*. Paper presented at the the Dynamics and Mass Budget of Arctic Glaciers. Extended Abstracts, Obergurgl (Austria).

Grześ, M., Król, M., & Sobota, I. (2009). Submarine evidence of the Aavatsmark and Dahl Glaciers fluctuations in the Kaffiøyra region, NW Spitsbergen. *Polish Polar Research*, 30(2), 143–160.

Hagen, J. O., Liestøl, O., Roland, E., & Jorgensen, T. (1993). Glacier atlas of Svalbard and Jan Mayen. Norsk Polarinstitutt. Meddelelser, 129.

Hooke, R. L. B. (2005). *Principles of glacier mechanics* (2nd ed., 429 pp.). Cambridge: Cambridge University Press. https://doi.org/10.1017/CBO9780511614231

Howat, I. M., Joughin, I., Tulaczyk, S., & Gogineni, S. (2005). Rapid retreat and acceleration of Helheim Glacier, east Greenland. *Geophysical Research Letters*, 32, L22502. https://doi.org/10.1029/2005GL024737

Jania, J., Perski, Z., & Stober, M. (2002). *Changes of geometry and dynamics of NW Spitsbergen glaciers based on the ground GPS survey and remote sensing*. Paper presented at the The changing physical environment. Proceedings from the Sixth Ny-Ålesund International Scientific Seminar Polar Environmental Centre, Tromsø.

Jiskoot, H., Murray, T., & Boyle, P. (2000). Controls on the distribution of surge-type glaciers in Svalbard. *Journal of Glaciology*, 46(154), 412–422. https://doi.org/10.3189/172756500781833115

Joughin, I., Abdalati, W., & Fahnestock, M. (2004). Large fluctuations in speed on Greenland's Jakobhavn Isbrae glacier. *Nature*, 432(7017), 608–610. https://doi.org/10.1038/nature03130

Kamb, B. (1987). Glacier surge mechanism based on linked cavity configuration of the basal water conduit system. *Journal of Geophysical Research*, 92, 9083–9100. https://doi.org/10.1029/JB092iB09p09083

Kamb, B., Raymond, C. F., Harrison, W. D., Engelhardt, H., Echelmeyer, K. A., Humphrey, N., et al. (1985). Glacier surge mechanism: 1982–1983 surge of the Variegated Glacier, Alaska. *Science*, 227(4686), 469–479. https://doi.org/10.1126/science.227.4686.469

König, M., Nuth, C., Kohler, J., Moholdt, G., & Pettersen, R. (2013). A digital glacier database for Svalbard. Ch. 10. In *Global Land Ice Measurements from Space*. Berlin: Praxis-Springer.

Korona, J., Berthier, R., Bernard, M., Rémy, F., & Thouvenot, E. (2009). SPIRIT. SPOT 5 stereoscopic survey of polar ice: Reference images and topographies during the fourth International Polar Year (2007–2009). *ISPRS J Photogramm*, 64(2), 204–212. https://doi.org/10.1016/j.isprsjprs.2008.10.005

Lankauf, K. R. (1999). *Retreat of the Aavatsmark Glacier (Kaffiöyra Region, Oscar II Land, Spitsbergen) in XX Century*. Paper presented at the XXVI Polar Symposium, Lublin.

Liestøl, O. (1969). Glacier surges in West Spitsbergen. *Canadian Journal of Earth Sciences*, 6(4), 895–897. https://doi.org/10.1139/e69-092

Lindbäck, K., Pettersson, R., Doyle, S. H., Helanow, C., Jansson, P., Kristensen, S. S., et al. (2014). High-resolution ice thickness and bed topography of a land-terminating section of the Greenland Ice Sheet. *Earth System Science Data*, 6(2), 331–338. https://doi.org/10.5194/essd-6-331-2014

Luckman, A., Benn, D. I., Cottier, F., Bevan, S., Nilsen, F., & Inall, M. (2015). Calving rates at tidewater glaciers vary strongly with ocean temperature. *Nature Communications*, 6(1), 8566. https://doi.org/10.1038/ncomms9566

Luckman, A., Murray, T., & Strozzi, T. (2002). Surface flow evolution throughout a glacier surge measured by satellite radar interferometry. *Geophysical Research Letters*, 29(23), 2095. https://doi.org/10.1029/2001GL014570

Mansell, D., Luckman, A., & Murray, T. (2012). Dynamics of tidewater surge-type glaciers in northwest Svalbard. *Journal of Glaciology*, 58(207), 110–118. https://doi.org/10.3189/2012JoG11J058

McMillan, M., Shepherd, A., Gourmelen, N., Dehecq, A., Leeson, A., Ridout, A., et al. (2014). Rapid dynamic activation of a marine-based Arctic ice cap. *Geophysical Research Letters*, 41, 8902–8909. https://doi.org/10.1002/2014GL062255

McNabb, R. W., & Hock, R. (2014). Alaska tidewater glacier terminus positions, 1948–2012. *Journal of Geophysical Research: Earth Surface*, 119, 153–167. https://doi.org/10.1002/2013JF002915

Meier, M. F., & Post, A. (1969). What are glacier surges? *Canadian Journal of Earth Sciences*, 6(4), 807–817. https://doi.org/10.1139/e69-081

Moholdt, G., Nuth, C., Hagen, J. O., & Kohler, J. (2010). Recent elevation changes of Svalbard glaciers derived from ICESat laser altimetry. *Remote Sensing of Environment*, 114(11), 2756–2767. https://doi.org/10.1016/j.rse.2010.06.008

Moon, T., & Joughin, I. (2008). Changes in ice front position on Greenland's outlet glaciers from 1992 to 2007. *Journal of Geophysical Research*, 113, F02022. https://doi.org/10.1029/2007JF000927

Murray, T., Dowdeswell, J. A., Drewry, D. J., & Frearson, R. (1998). Geometric evolution and ice dynamics during a surge of Bakaninbreen, Svalbard. *Journal of Glaciology*, 44(147), 263–272. https://doi.org/10.1017/S0022143000002604

Murray, T., James, T. D., Macheret, Y. Y., Lavrentiev, I., Glazovsky, A., & Sykes, H. (2012). Geometric changes in a tidewater glacier in Svalbard during its surge cycle. *Arctic, Antarctic, and Alpine Research*, 44(3), 359–367. https://doi.org/10.1657/1938-4246-44.3.359

Murray, T., Luckman, A., Strozzi, T., & Nuttall, A. M. (2003). The initiation of glacier surging at Fridtjovbreen, Svalbard. *Annals of Glaciology*, 36(1), 110–116. https://doi.org/10.3189/172756403781816275

Murray, T., Strozzi, T., Luckman, A., Jiskoot, H., & Christakos, P. (2003). Is there a single surge mechanism? Contrasts in dynamics between glacier surges in Svalbard and other regions. *Journal of Geophysical Research*, 108(B5), 2237. https://doi.org/10.1029/2002jb001906

Murray, T., Stuart, G. W., Miller, P. J., Woodward, J., Smith, A. M., Porter, P. R., & Jiskoot, H. (2000). Glacier surge propagation by thermal evolution at the bed. *Journal of Geophysical Research*, 105, 13,491–13,507. https://doi.org/10.1029/2000JB900066

Navarro, F. J., & Eisen, O. (2009). Ground-penetrating radar. In P. Pilleka & W. G. Rees (Eds.), *Remote sensing of glaciers: Techniques for topographic, spatial and thematic mapping of glaciers* (pp. 195–230). London: Taylor & Francis.

Nick, F. M., Vieli, A., Howat, I. M., & Joughin, I. (2009). Large-scale changes in Greenland outlet glacier dynamics triggered at the terminus. *Nature Geoscience*, 2(2), 110–114. https://doi.org/10.1038/ngeo394

Niewiarowski, W. (1982). Morphology of the forefield of the Aavatsmark Glacier (Oscar II Land, NW Spitsbergen) and phases of its formation. In *Acta Univ. N. Copernici, Geografia XVI, Toruń* (pp. 147–158).

Norwegian Polar Institute (2014). *Terrengmodell Svalbard (S0 Terrengmodell)*. Tromsø, Norway: Norwegian Polar Institute. Retrieved from https://geodata.npolar.no

Nuth, C., & Kääb, A. (2011). Co-registration and bias corrections of satellite elevation data sets for quantifying glacier thickness change. *The Cryosphere*, 5(1), 271–290. https://doi.org/10.5194/tc-5-271-2011

Nuth, C., Kohler, J., König, M., von Deschwanden, A., Kääb, A., Moholdt, G., & Pettersson, R. (2013). Decadal changes from a multi-temporal glacier inventory of Svalbard. *The Cryosphere*, 7(5), 1603–1621. https://doi.org/10.5194/tc-7-1603-2013

Nuth, C., Moholdt, G., Hagen, J. O., & Kääb, A. (2010). Svalbard glacier elevation changes and contribution to sea level rise. *Journal of Geophysical Research*, 115, F01008. https://doi.org/10.1029/2008JF001223

O'Neel, S., Pfeffer, W. T., Krimmel, R. M., & Meier, M. F. (2005). Evolving force balance at Columbia glacier, Alaska, during its rapid retreat. *Journal of Geophysical Research*, 110, F03012. https://doi.org/10.1029/2005JF000292

Palmer, S., Shepherd, A., Nienow, P., & Joughin, I. (2011). Seasonal speedup of the Greenland Ice Sheet linked to routing of surface water. *Earth and Planetary Science Letters*, 302(3–4), 423–428. https://doi.org/10.1016/j.epsl.2010.12.037

Pettersson, R., Jansson, P., Huwald, H., & Blatter, H. (2007). Spatial pattern and stability of the cold surface layer of Storglaciären, Sweden. *Journal of Glaciology*, 53(180), 99–109. https://doi.org/10.3189/172756507781833974

Pfeffer, T., Arendt, A. A., Bliss, A., Bolch, T., Cogley, J. G., Gardner, A. S., et al. (2014). The Randolph Glacier Inventory, a globally complete inventory of glaciers. *Journal of Glaciology*, *60*(221), 537–552. https://doi.org/10.3189/2014JoG13J176

Plassen, L., Vorren, T. O., & Forwick, M. (2004). Integrated acoustic and coring investigation of glacigenic deposits in Spitsbergen fjords. *Polar Research*, *23*(1), 89–110. https://doi.org/10.3402/polar.v23i1.6269

Rippin, D. M., Carrivick, J. L., & Williams, C. (2011). Evidence towards a thermal lag in the response of Kårsaglaciären, northern Sweden, to climate change. *Journal of Glaciology*, *57*(205), 895–903. https://doi.org/10.3189/002214311798043672

Rolstad, C., Amlien, J., Hagen, J. O., & Lundén, B. (1997). Visible and near-infrared digital images for determination of ice velocities and surface elevation during a surge on Osbornebreen, a tidewater glacier in Svalbard. *Annals of Glaciology*, *24*, 255–261. https://doi.org/10.1017/S026030550001226X

Rott, H., & Nagler, T. (1994). *Capabilities of ERS-1 SAR for snow and glacier monitoring in Alpine areas*. Paper presented at the Proceedings of the 2nd ERS-1 Symposium SP-361.

Sevestre, H., & Benn, D. (2015). Climatic and topographic controls on the global distribution of surge-type glaciers: Implications for a unifying model of surging. *Journal of Glaciology*, *61*(228), 646–662. https://doi.org/10.3189/2015JoG14J136

Sevestre, H., Benn, D. I., Hulton, N. R. J., & Bælum, K. (2015). Thermal structure of Svalbard glaciers and implications for thermal switch models of glacier surging. *Journal of Geophysical Research: Earth Surface*, *120*, 2220–2236. https://doi.org/10.1002/2015JF003517

Sobota, I. (2013). Współczesne zmiany kriosfery północno-zachodniego Spitsbergenu na przykładzie region PhD, Universytety Mikolaja Kopernika.

Sobota, I., Weckwerth, P., & Nowak, M. (2016). Surge dynamics of Aavatsmarkbreen, Svalbard, inferred from the geomorphological record. *Boreas*, *45*(2), 360–376. https://doi.org/10.1111/bor.12160

Sole, A., Mair, D. W. F., Nienow, P. W., Bartholomew, I. D., King, M. A., Burke, M. J., & Joughin, I. (2011). Seasonal speedup of a Greenland marine-terminating outlet glacier forced by surface melt–induced changes in subglacial hydrology. *Journal of Geophysical Research*, *116*, F03014. https://doi.org/10.1029/2010JF001948

Sund, M., Eiken, T., Hagen, J. O., & Kääb, A. (2009). Svalbard surge dynamics derived from geometric changes. *Annals of Glaciology*, *50*(52), 50–60. https://doi.org/10.3189/172756409789624265

van der Veen, K. (2017). *Fundamentals of glacier dynamics* (2nd ed.). Balkema, Rotterdam.

Wilson, N. J., Flowers, G. E., & Mingo, L. (2013). Comparison of thermal structure and evolution between neighboring subarctic glaciers. *Journal of Geophysical Research: Earth Surface*, *118*, 1443–1459. https://doi.org/10.1002/jgrf.20096

Zwally, H. J., Abdakati, W., Herring, T., Larson, K., Saba, J., & Steffen, K. (2002). Surface melt-induced acceleration of Greenland Ice Sheet flow. *Science*, *297*(5579), 218–222. https://doi.org/10.1126/science.1072708